Rethinking Image Deraining via Rain Streaks and Vapors

Anonymous ECCV submission

Paper ID 2761

1 Comparisions with [7] and [1]

In order to let the images in our paper have larger sizes, so that some details can be seen more clearly, the comparisons with [7] and [1] are reported here. The objective indexes on our two datasets are shown in Table 1 and 2. Running time comparisons are in Table 3. Fig. 1 is the visual results on the synthetic rainy images which appear in our paper. Fig. 2 is the visual results on the real-world rainy images which appear in our paper. More comparisons with all the selected methods and some other relative results are shown in the later sections in this document.

2 Localization of Rain

In Section 3.4.1 in our paper, we need to locate the rainy pixels before pretraining our ANet. We utilize the method in [5] to detect rainy pixels. Because the authors utilize Softmax to approximate the binary location map, we implement binarization to their results in our work, some results are shown in Fig. 3.

3 More Comparisons with Selected Methods on Synthetic Rainy Images

We also show more visual comparisons on different types of synthetic rainy images. Except for the four state-of-the-art works used in our paper, here we add another two works [1] and [7] to make comparisons. The synthetic rainy images which come from [1] by Fu et al., [3] by Li et al. and [7] by Zhang et al. are shown in Fig. 4. The rain streaks by Yang et al. [5] are really bright. In Fig. 5 we show another 6 synthetic rainy images from Rain100H by Yang et al.. It can be seen that our method obtains better rain-removed visual effect on this dataset.

4 More Comparisons with Selected Methods on Real-World Rainy Images

In Fig. 6, 7, 8, 9 and 10, we show more results for real-world rainy images. We can see that our method outperforms other state-of-the-art methods in removing rain effect. The work [2] cannot remove rain streaks well for some images and it may change the color

Table 1. PSNR/SSIM comparisons of [7], [1] and our methods on our two datasets

Methods	[1]	[7]	Ours
Rain-I	29.10/0.873	26.66/0.885	**31.34/0.908**
Rain-II	30.01/0.895	25.33/0.867	**34.42/0.938**

Table 2. FID comparisons of [7], [1] and our methods on our two datasets

Methods	[1]	[7]	Ours
Rain-I	59.66	65.51	**50.66**
Rain-II	80.44	88.34	**67.18**

hue of original rainy images, e.g., the second and third in Fig. 10, so that some abnormal hue appears in the deraining results. Besides, this work may produce blocking effect for some rainy images, e.g., the fourth one in Fig. 6. For some rainy images, existing methods may lose image details, e.g., the first, second, and third in Fig. 7. Please zoom in to see clearly. We will release our code, all the other rainy images can be tested.

5 More Comparisons with Selected Methods on A Rainy Video

We also apply the state-of-the-art and our methods on a rainy video with heavy rain. We can see that the work [2] and our method produce better deraining results. Compared with [2], our method removes rain streaks more clearly, especially the bright streaks in some successive frames. For some frames, [2] removes more vapor than ours, but this work changes the color hue of the video, i.e., the colors of the deraining result are different from that of original video, especially, the house becomes green dring the fifth and nineth seconds. The colors of house are mixed with that of the green things around it, which may be due to the extracted global features when learning transmission of vapor from the low-frequency pass.

References

1. Fu, X., Huang, J., Zeng, D., Huang, Y., Ding, X., Paisley, J.: Removing rain from single images via a deep detail network. In: IEEE Conference on Computer Vision and Pattern Recognition (CVPR-2017). pp. 1715–1723. IEEE, Honolulu, HI, USA (July 2017)
2. Li, R., Cheong, L.F., Tan, R.T.: Heavy rain image restoration: Integrating physics model and conditional adversarial learning. In: IEEE Conference on Computer Vision and Pattern Recognition (CVPR 2019). IEEE, Long Beach CA, USA (Jun 2019)
3. Li, X., Wu, J., Lin, Z., Liu, H., Zha, H.: Recurrent squeeze-and-excitation context aggregation net for single image deraining. In: European Conference on Computer Vision (ECCV-2018). IEEE, Munich, Germany (Sep 2018)
4. Wang, T., Yang, X., Xu, K., Chen, S., Zhang, Q., Lau, R.W.: Spatial attentive single-image deraining with a high quality real rain dataset. In: IEEE Conference on Computer Vision and Pattern Recognition (CVPR 2019). IEEE, Long Beach CA, USA (Jun 2019)

Table 3. Average complexity comparisons of [7], [1] and our methods on our two datasets. The image size is 512×512

Methods	[1]	[7]	Ours
Time	$0.09s$	$0.06s$	$0.03s$

(a) Input (b) [1] (c) [7] (d) Ours (e) GT

Fig. 1. Qualitative comparisons of selected methods and our method on synthetic rainy images. (a) Input rainy images. (b)-(d) Deraining results of DDN [1], DID-MDN [7], and our method. (e) Ground truth. These two samples are two failure cases of the state-of-the-art methods.

5. Yang, W., Tan, R.T., Feng, J., Liu, J., Guo, Z., Yan, S.: Deep joint rain detection and removal from a single image. In: IEEE Conference on Computer Vision and Pattern Recognition (CVPR-2017). pp. 1685–1694. IEEE, Honolulu, HI, USA (July 2017)
6. Yang, W., Tan, R.T., Feng, J., Liu, J., Yan, S., Guo, Z.: Joint rain detection and removal from a single image with contextualized deep networks. IEEE Transactions on Pattern Analysis and Machine Intelligence (January 2019)
7. Zhang, H., Patel, V.M.: Density-aware single image de-raining using a multi-stream dense network. In: IEEE Conference on Computer Vision and Pattern Recognition (CVPR-2018). pp. 1685–1694. IEEE, Salt Lake City, UT (July 2018)

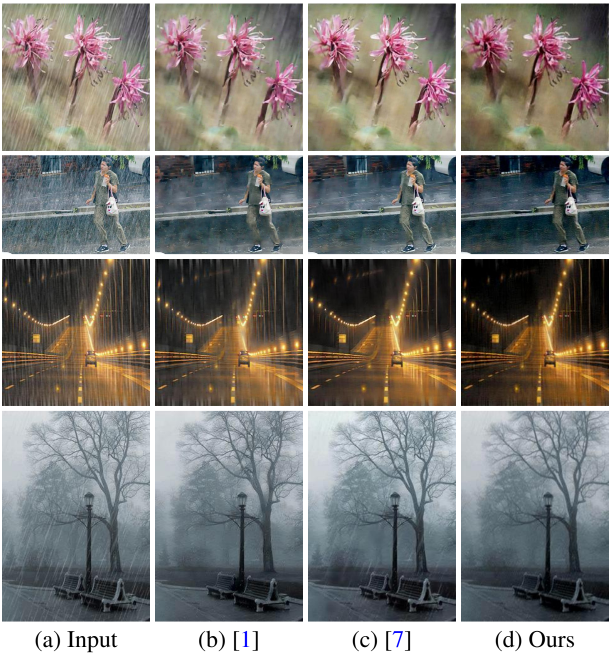

Fig. 2. Qualitative comparisons of selected methods and our method on real-world rainy images. (a) Input rainy images. (b)-(d) Deraining results of DDN [1], DID-MDN [7], and our method.

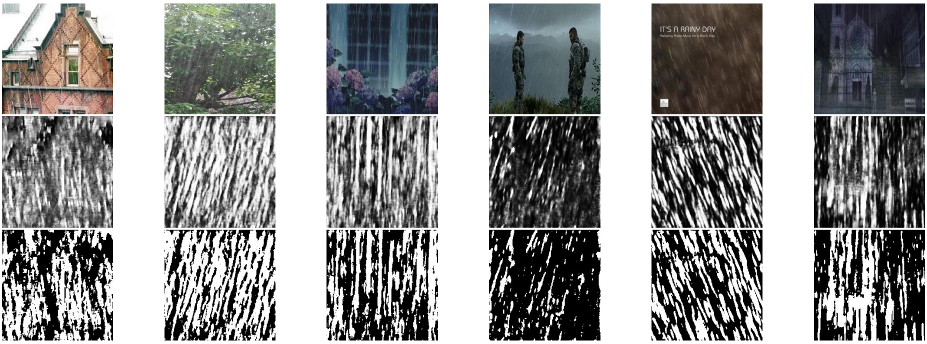

Fig. 3. This figure shows some results of detecting rainy pixels: the first line is the rainy images, the second line is the results by [5], the third line is the results by binarization, the threshold in our work is 0.5.

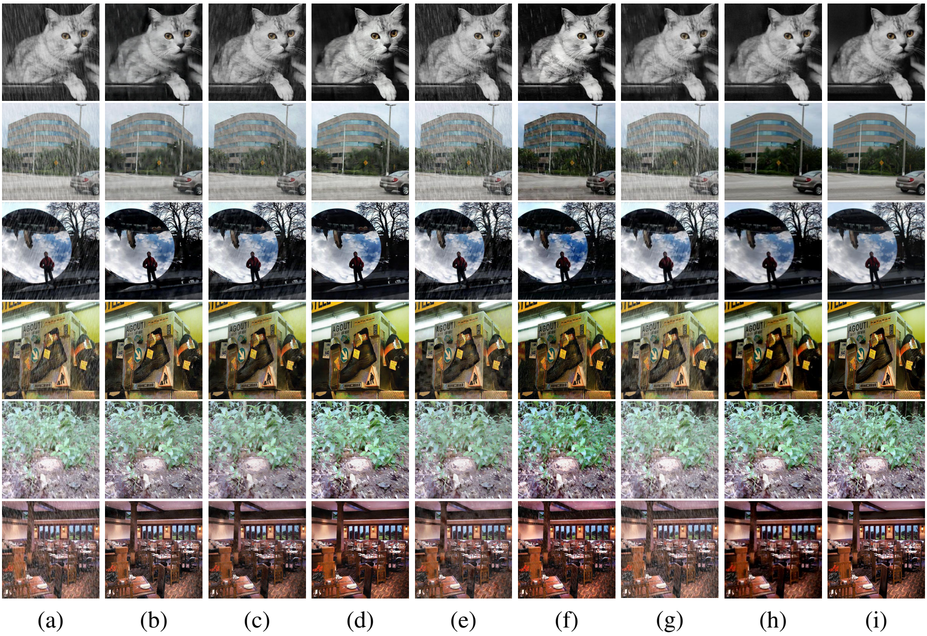

Fig. 4. This figure shows more results of selected and our methods on synthetic rainy images. (a) Input. (b)-(h) Deraining results of [1], [3], [7], [6], [2], [4] and ours. (i) Ground Truth. The first rainy image comes from the dataset of [1] by Fu et al., the second and third images come from [3] by Li et al., the last three images come from [7] by Zhang et al..

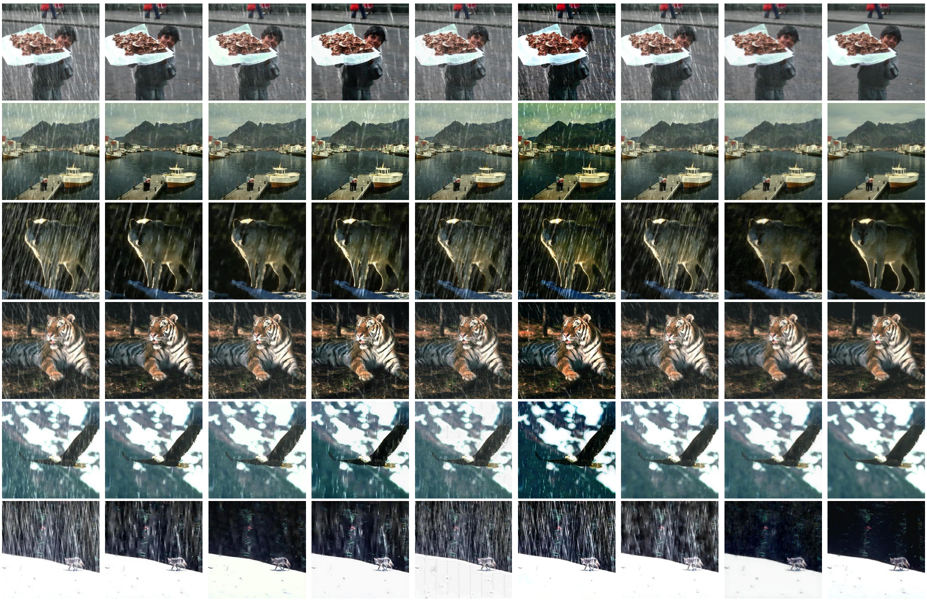

(a) (b) (c) (d) (e) (f) (g) (h) (i)

Fig. 5. This figure shows more results of selected and our methods on the dataset from [5]. (a) Input. (b)-(h) Deraining results of [1], [3], [7], [6], [2], [4] and ours. (i) Ground Truth.

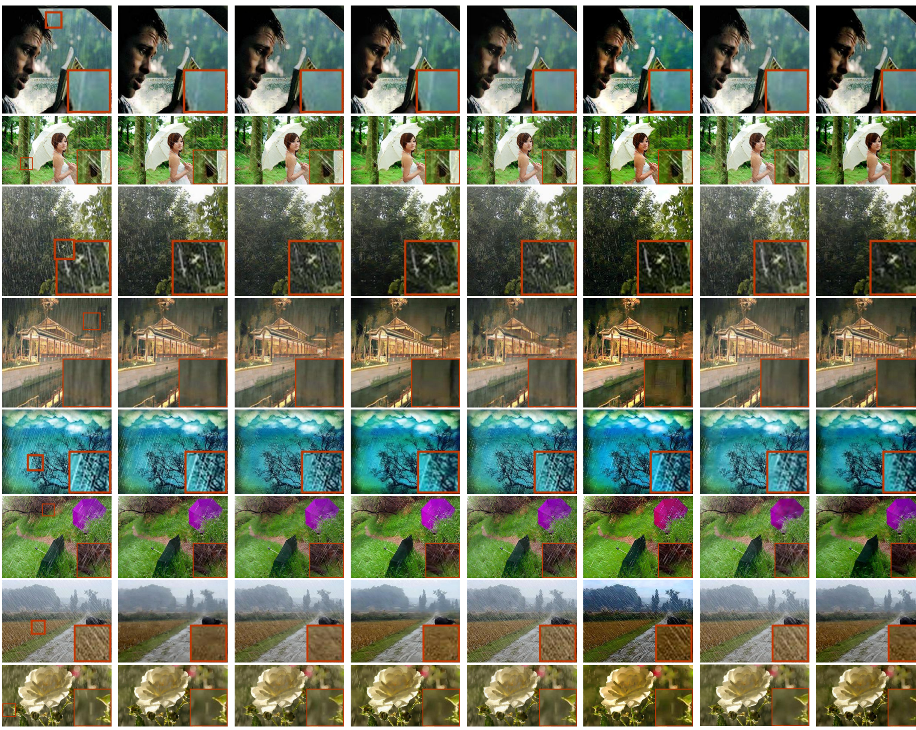

(a) (b) (c) (d) (e) (f) (g) (h)

Fig. 6. This figure shows more results of the selected and our methods on real-world rainy images. (a) Input. (b)-(h) Deraining results of [1], [3], [7], [6], [2], [4] and ours.

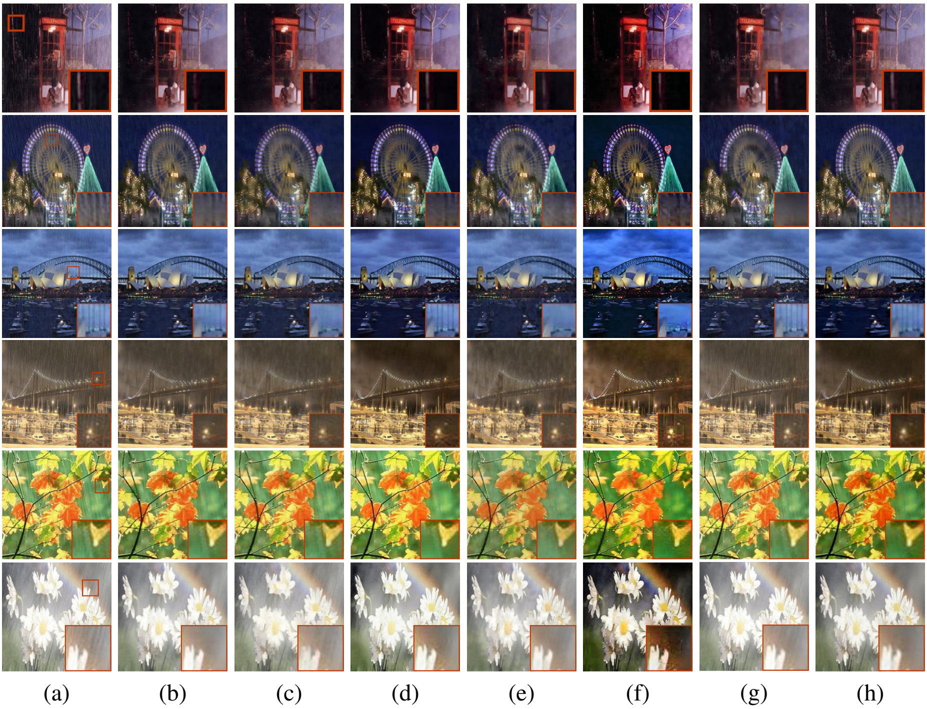

Fig. 7. This figure shows more results of the selected and our methods on real-world rainy images. (a) Input. (b)-(h) Deraining results of [1], [3], [7], [6], [2], [4] and ours.

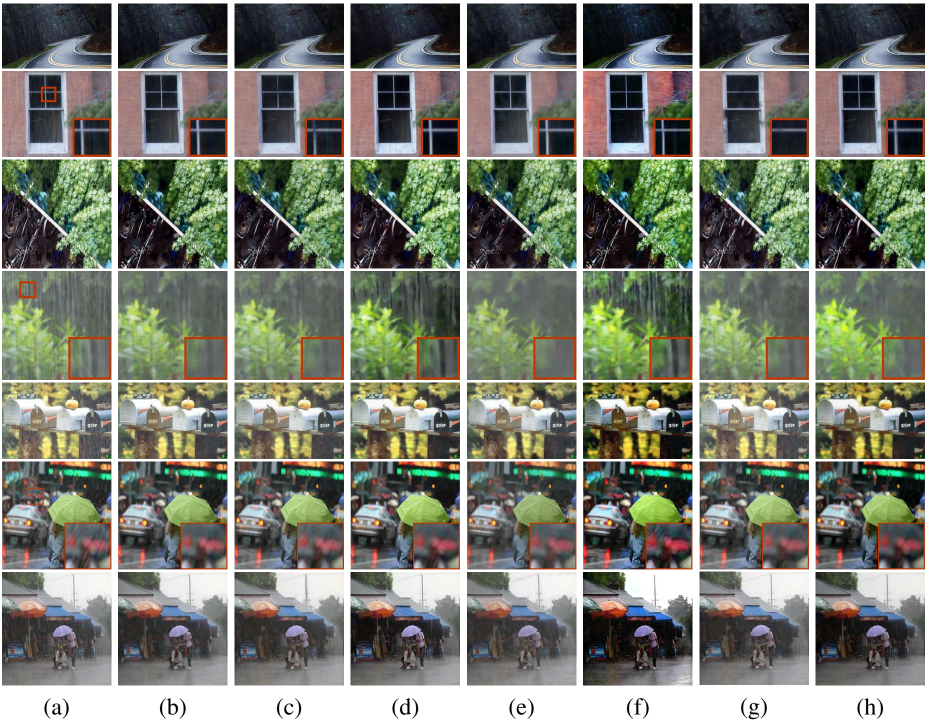

Fig. 8. This figure shows more results of the selected and our methods on real-world rainy images. (a) Input. (b)-(h) Deraining results of [1], [3], [7], [6], [2], [4] and ours.

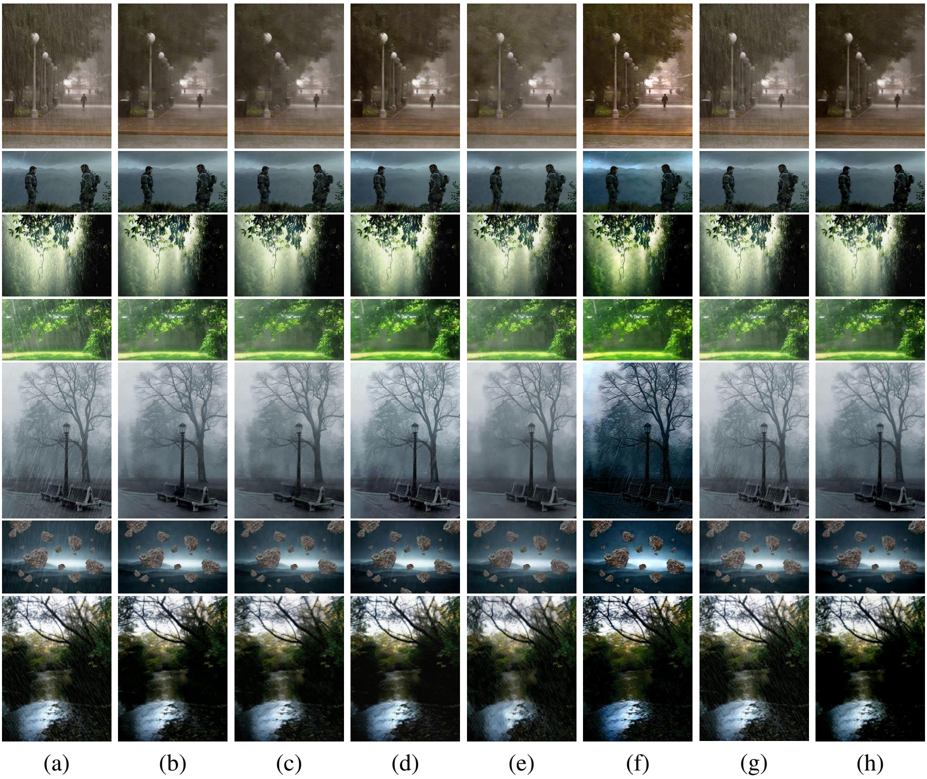

Fig. 9. This figure shows more results of the selected and our methods on real-world rainy images. (a) Input. (b)-(h) Deraining results of [1], [3], [7], [6], [2], [4] and ours.

(a) (b) (c) (d) (e) (f) (g) (h)

Fig. 10. This figure shows more results of the selected and our methods on real-world rainy images. (a) Input. (b)-(h) Deraining results of [1], [3], [7], [6], [2], [4] and ours.